Taylor & Francis
healthsciences

S P E C I A L   R E P O R T

A clinicopathological study of three cases of severe acute respiratory syndrome (SARS)

Zhen-Wei Lang*, Li-Jie Zhang*, Shi-Jie Zhang*, Xin Meng*, Jun-Qiang Li*, Chen-Zhao Song*, Ling Sun*, Yu-Sen Zhou* and Dominic E. Dwyer†‡

*Department of Pathology, Beijing Youan Hospital, Capital University of Medical Sciences, China, †World Health Organisation China, Chaoyang District, Beijing, China and ‡Centre for Infectious Diseases and Microbiology Laboratory Services, ICPMR, Westmead Hospital, Westmead, Australia

Summary

Aims: The severe acute respiratory syndrome (SARS) caused a large outbreak of atypical pneumonia in Beijing, China from early March 2003. We report the pathological features from three patients who died of SARS.

Methods: Autopsies were performed on three patients who died 9–15 days after the onset of the illness, and the clinical and laboratory features reviewed. Tissue sections were stained with haematoxylin and eosin (H&E), and *in situ* reverse transcriptase polymerase chain reaction (RT–PCR) on lung sections was performed using SARS coronavirus-specific primers.

Results: The typical gross pathological change in the lungs was diffuse haemorrhage on the lung surface. Histopathological examination revealed serous, fibrinous and haemorrhagic inflammation in most pulmonary alveoli, with capillary engorgement and some capillary microthrombosis. The pulmonary alveoli were thickened with interstitial mononuclear inflammatory infiltrates, diffuse alveolar damage, desquamation of pneumocytes and hyaline-membrane formation; fibrinoid material and erythrocytes were present in alveolar spaces. There were thromboemboli in some bronchial arterioles. Haemorrhagic necrosis and reduced numbers of lymphocytes were observed in lymph nodes and spleen. *In situ* RT–PCR detected SARS coronavirus RNA in type II alveolar cells, interstitial cells and bronchiolar epithelial cells from all three patients.

Conclusions: Severe immunological damage in lung tissue is responsible for the clinical features of SARS.

INTRODUCTION

The severe acute respiratory syndrome (SARS) has affected over 8 400 people worldwide, with most cases in China, Taiwan, Hong Kong Special Administrative Region (HK SAR), Singapore and Canada.[1] The largest outbreak worldwide has occurred in Beijing, China with over 2 500 cases. The causative agent is a novel coronavirus, which has not been detected previously in human populations. It has been isolated in culture and detected by electron microscopy and reverse transcriptase polymerase chain reaction (RT–PCR) from a range of clinical specimens. In addition, serological evidence of infection has been found in most patients fitting the clinical definition of SARS, although antibody responses may be slow to develop.[2–5] The genome of the SARS coronavirus (SARS–CoV) has been sequenced from multiple clinical isolates.[6]

SARS is fatal in at least 10% of cases, with a higher mortality in the elderly or where the person has underlying diabetes, heart or lung disease, or impaired immunity.[5,7,8] An understanding of the pathogenesis and histopathological features of SARS–CoV infection is essential to the management of the disease.

During the SARS outbreak in Beijing, 200 patients with suspected/probable SARS were admitted to Youan Hospital, Beijing (a designated SARS hospital during the outbreak) from 9 March to 9 April 2003, of whom 15 died within two weeks of onset of the illness. We performed autopsies on three patients and report the pathological characteristics of these cases.

PATIENTS AND METHODS

Patients

Patient 1 was a 73-year-old man with a medical history of lung cancer who came to Beijing from Shanxi province and died nine days after the onset of his illness. He presented with a self-reported fever of 38.5°C, chills, dyspnoea and a minimally productive cough. Laboratory studies included a white blood cell (WBC) count of 1.9×10^9/L with 28% lymphocytes. A chest radiograph showed interstitial infiltrates in both left and right lungs. He had had contact with a patient with atypical pneumonia before his hospitalisation. He had received 400 mg of methylpredisolone during the five days before death.

Patient 2 was a 64-year-old woman with diabetes who died 15 days after onset of her illness.

Patient 3 was a 69-year-old woman with diabetes, hypertension and heart disease who died 13 days after the onset of her illness.

Patients 2 and 3 were both hospitalised with a high fever (39°C), chills and dyspnoea. Laboratory studies included a WBC of 3.7×10^9/L with 16% lymphocytes in Patient 2 and 5.7×10^9/L with 8% lymphocytes in Patient 3. Chest radiographs showed interstitial infiltrates in the lower and middle zones of the lungs for both patients. Patients 2 and 3 both lived in Beijing. Prior to her hospitalisation, Patient 2 had a history of contact with a family member who had a fever and a cough, whereas Patient 3 reported contact with an unrelated individual with fever and cough.

Autopsies

All three patients had post-mortem examinations performed, with the pathological changes studied by microscopy. The clinical data were reviewed. Autopsy specimens were fixed in 4% neutral buffered formalin and embedded in paraffin; 4 μm-thick sections were stained with H&E. To minimise potential SARS–CoV transmission, no further autopsies were undertaken from April 2003.

Detection of SARS–CoV RNA by in situ RT–PCR

Three SARS–CoV specific primers were designed from an early SARS–CoV isolate (Genbank accession number AY278554), targeting the SARS–CoV *polymerase* gene in open reading frame 1b. These were sense primers cor-F2 5′-CTAACATGCTTAGGATAATGG-3′ (15235-15235) and cor-F3 5′-GCCTCTCTTGTTCTTGCTCGC-3′ (15255–15275), and the antisense primer cor-R1 5′-CAGGTAAGCGTAAAACTCATC-3′ (15602-15582). The cor-F2-cor-R1 primer pair generates a 368 base pair PCR amplicon, and the cor-F3-cor-R1 primer pair generates a 348 base pair PCR amplicon (Genbank accession number AY278554).

Five-micrometre sections were deparaffinised, rehydrated, and digested with proteinase K (30 μg/ml) for 15 minutes at 37°C, followed by reverse transcription (RT). The RT reaction mixture contained 4 μl 5 × first round buffer, 1 μl of 0.5 μg/μl oligo dT (Promega Corporation, Madison, WI, USA), 1 μl of 10 mM dNTP, 2 μl of 0.1M dithiothreitol (dTT), 1 μl of 40 u/μl RNasin and 1 μl of Moloney murine leukemia virus (MMLV) reverse transcriptase (200 U//μl Gibco BRL, Gaithersburg, MD, USA) and diethylpolycarbonate (DEPC)-treated H$_2$O to a final reaction volume of 20 μl. The 20 μl mixture was added to each section and the slides placed in a moist chamber for a 60-minute incubation at 37°C. The reaction was terminated by heating at 70°C for 15 minutes.

The PCR mixture contained 4 μl 10 × PCR buffer (Invitrogen, Groningen, The Netherlands), 2 μl digoxigenin (dig)-dNTPs (Roche Diagnostics, Mannheim, Germany), 1 μl each of the cor-F3 and cor-R1 primers, 0.5 μl *Taq* polymerase (Sigma, St Louis, MO, USA) and DEPC-treated H$_2$O to a 40 μl total volume. The residual fluid was gently decanted from the slides and the 40 μl PCR mixture added to each slide. The slides were covered with a clean coverslip and cemented with wax oil. Thermal cycling parameters were a single cycle of 95°C denaturation for 3 minutes, then 20 cycles at 95°C for 50 seconds and 68°C for 3 minutes, followed by a final reaction extension at 72°C extension for 5 minutes. To ensure specificity, dNTP instead of dig-dNTP was used as a negative control.

Wax oil on the slides was cleared with xylene and the coverslips carefully removed. The tissue samples were fixed by adding 4% poly-formaldehyde and acetic anhydride/triethanolamine, and blocked by goat serum. Anti-digoxigenin-AP (1:500) antibody was added to the samples on slides and incubated at 37°C for 60 minutes. Slides were washed gently. Nitroblue tetrazolium/5-bromo-4-chloro-3-indole-phosphate (NBT/BCIP) (Promega Corporation, Madison, WI, USA) staining solution was added to the slides and examined. The slides were sealed with glycerol.

RESULTS

Laboratory Testing

Baseline full blood count, biochemistry, liver function tests, coagulation studies and CD4+ and CD8+ T lymphocyte counts (measured by flow cytometry) are listed in Table 1. Of note was the low WBC count, neutropenia, thrombocytopenia and lymphopenia (CD4+ and CD8+ cells), in addition to marked hyponatremia. The patients had not received ribavirin therapy. Convalescent sera were not available from these patients for SARS–CoV-specific antibody testing.

Gross Pathology

There was a small amount of pink or red fluid in the thoracic cavity, without evidence of pleural adhesions, seen in the three patients. The lungs displayed surface erythema and were firm to touch (Fig. 1). The lungs all floated on water. There was a small amount of pink or red fluid when the lungs were cut. Red serous fluid was observed in the bronchi and respiratory tract of all patients.

Histopathology

Nearly every lobe of the lungs from each patient showed diffuse serous inflammation. The alveolar capillaries were markedly expanded with hyperaemia. The alveolar walls were oedematous with a combined lymphocytic and mononuclear cell infiltrate. There was active proliferation of Type II alveolar epithelial cells and interstitial cells. A light red-coloured, homogeneous fibrinous deposition was observed on the alveolar walls. The capillary basement membranes were thickened and expanded from the pulmonary alveolar walls. There was desquamation of pneumocytes and a light-red exudative fluid containing fibrin, red blood cells (RBC), macrophages and epithelial

TABLE 1 Baseline laboratory results

Parameters (normal range)	Patient 1	Patient 2	Patient 3
Haemoglobin (110–160 g/dL)	122	115	135
Platelets (100–300 × 10^9/L)	127	52	250
WBC (4–10 × 10^9/L)	1.9	3.7	5.7
Neutrophils (2–7.5 × 10^9/L)	1.25	2.4	3.8
Lymphocytes (0.8–4 × 10^9/L)	0.5	0.9	0.8
PT (10.5–14.5 seconds)	11.4	10.8	10.5
APPT (26–38 seconds)	35.7	36.0	30.5
Sodium (136–145 mmol/L)	131	131	130
Potassium (3.5–5.5 mmol/L)	3.7	4.1	2.5
Urea (2.29–7 mmol/L)	4.9	8.7	9.0
Creatinine (34–170 mmol/L)	nd	94	77
Bilirubin (0.3–1.2 mmol/L)	0.71	0.42	1.49
ALT (5–40 IU/L)	22	16	46
CD3+ cells (770–2041 × 10^6/L)	299	701	700
CD3+ CD4+ % (34–70%)	36	61	54
CD3+ CD4+ cells (414–1123 × 10^6/L)	107	426	381
CD3+ CD8+ % (25–54)	65	44	42
CD3+ CD8+ cells (238–874 × 10^6/L)	19	310	297
CD4+ CD8+ ratio (0.68–2.47)	0.56	1.38	1.28

Abbreviations: PT, prothrombin time; APTT, activated partial thromboplastin time; ALT, alanine transferase; nd, not done.

Fig. 1 Lung specimen taken from Patient 1 showing diffuse haemorrhage.

cells in many alveolar spaces (Fig. 2, 3). Hyaline-membrane formation was observed in some alveoli (Fig. 4). Viral-like inclusions were identified in Patients 1 and 2; these looked like homogeneous red-coloured bodies with a halo-like envelope on H & E staining (Fig. 5).

Typical large multinucleated syncytial cells were absent in all the three cases. We observed only a few multinucleated cells containing 3–4 nuclei. Other changes included bronchiolar submucosal oedema, inflammatory cell infiltrates, and desquamation and focal hyperplasia of epithelial cells. Many neutrophils and fibrous thrombi were found in the adjacent vessels (Fig. 6). No haemophagocytosis was seen, and there was no evidence of secondary bacterial pneumonia. Examination by electron microscopy was not performed.

The normal architecture of lung hilar lymph nodes was destroyed, with obvious expansion of lymphatic sinuses and vessels. The lymphocytes in the cortical regions were greatly reduced and the germinal centre lost. There was marked proliferation of macrophages in subcapsular sinuses. Vacuolated lipid was found in cytoplasmic spaces of macrophages (Fig. 7). Focal necrotic inflamma-

tion was present in the lymph nodes of the hilum of the lung, but not in any other lymph nodes. The spleens were soft and the splenic pulp was difficult to scrape down. The splenic changes included white pulp atrophy, depletion of lymphocytes around lymphatic sheaths, and reduced lymphocytes in the red pulp. Focal haemorrhagic necrotic inflammation was observed near the splenic capsule (Fig. 8).

The hepatocytes showed some oedema and fatty degeneration in liver lobules. There was active proliferation of Kupffer cells and the hepatic portals were swollen slightly with lymphocytic infiltrates (Fig. 9).

Pathological changes in heart tissues included atrophied cardiac muscle fibres with lipofuscin deposition in the cytoplasm, and some proliferation of interstitial cells and lymphocytes. The renal cortices were thin. The renal tubules displayed hydropic degeneration or swelling and some protein casts were present. In Patient 3, there was obvious glomerular fibrosis with corresponding tubular fibrosis and atrophy, leading to compensatory hypertrophy in remnant glomeruli. The acini of the pancreas were slightly atrophied with a mild lymphocytic infiltration. Most islets were atrophied with a pink matrix deposition in the pancreas of two patients. Adrenal glands showed
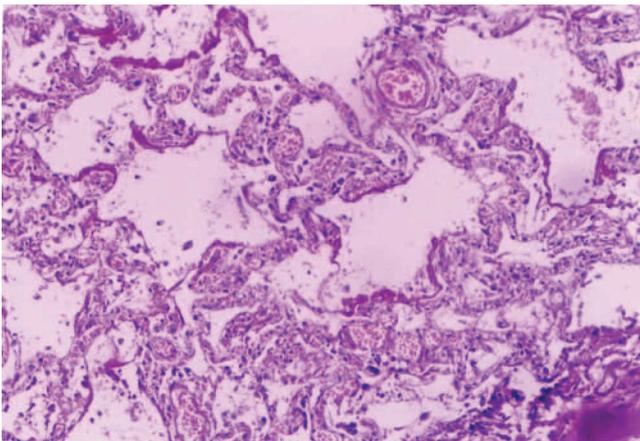

Fig. 2 Lung tissue from Patient 1 showing alveolar wall capillaries engorged with interstitial mononuclear cell infiltrates, with serous fluid, fibrin and RBC present in the alveolar spaces (H & E, original magnification, ×200).
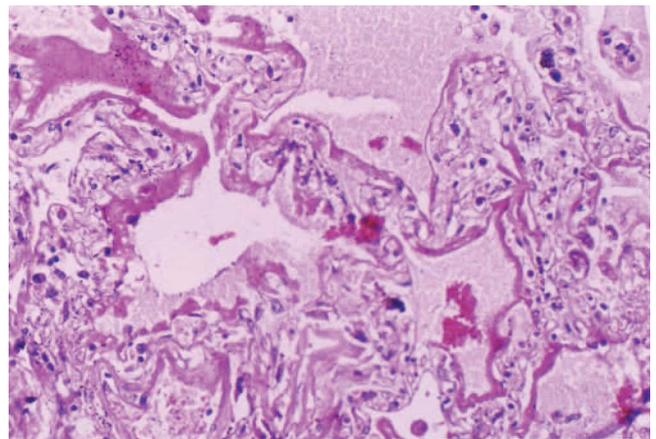

Fig. 4 Hyaline-membrane formation in alveolar spaces, seen in all three patients (H & E, original magnification, ×200).
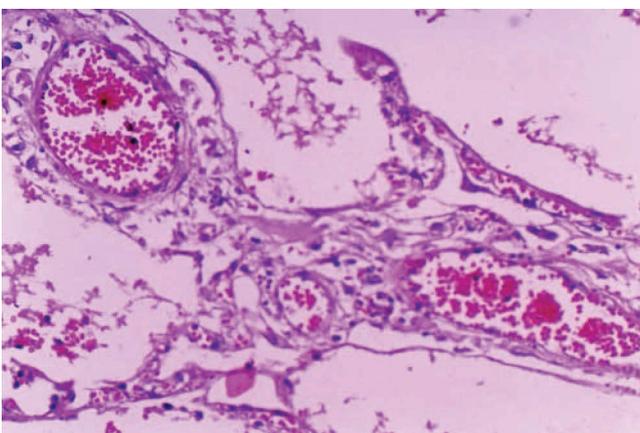

Fig. 3 Thickened capillary basement membranes and alveolar walls (Patient 1) (H & E, original magnification, ×200).
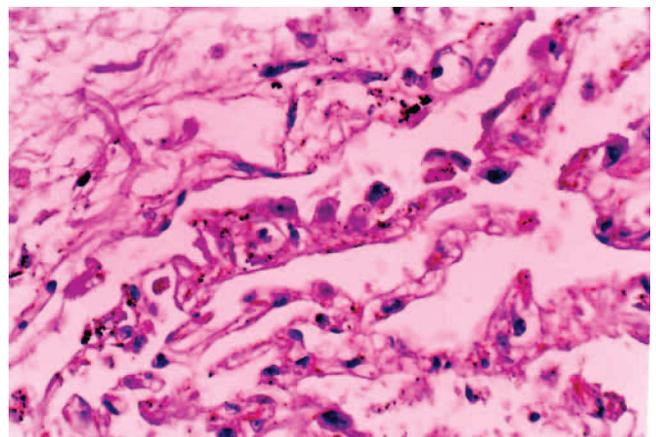

Fig. 5 Viral-like inclusions were identified in Patients 1 and 2; these appeared as homogeneous red-coloured bodies with a halo-like envelope (H & E, original magnification, ×200).
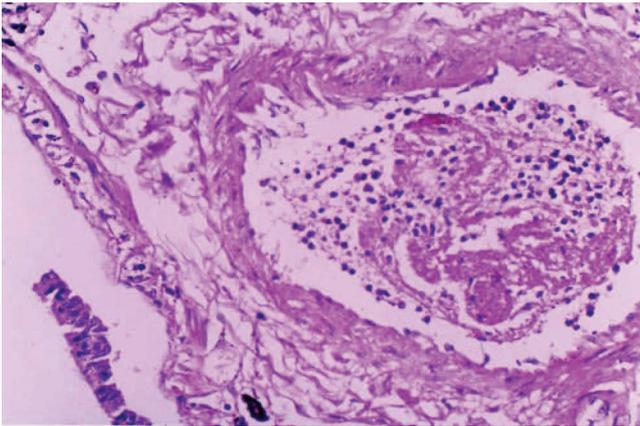
Fig. 6 Loss of the bronchiolar mucous membrane and blood vessels with fibrin thrombosis and mild neutrophil infiltrate (Patient 1) (H & E, original magnification, ×200).

Fig. 8 Splenic tissue showing loss of lymphocytes in splenic red pulp, with some haemorrhagic necrosis near the envelope zones (H & E, original magnification, ×200).

extensive haemorrhage and necrosis. The small intestine had no evidence of mucosal injury, hyperaemia and or submucosal oedema. There was submucosal distribution of lymphocytes. There was no pathological damage in the colon.

Molecular tests

SARS–CoV RNA was detected in lung tissue sections from the three patients. The positive signals were located in the Type II alveolar epithelial cells, interstitial cells and bronchiolar cells. The distribution of positive cells were scattered throughout the lung tissue (Fig. 10). The slides treated with dNTP instead of dig-dNTP were negative.

DISCUSSION

We describe the laboratory features and postmortem changes in different tissues from three patients who died during the SARS outbreak in Beijing. As expected, the predominant damage was evident in the lungs and was characterised by acute exudative and haemorrhagic

Fig. 9 Liver tissue showing slightly swollen hepatocytes with some fatty degeneration. There is proliferation of the Kupffer cells and some enlarged portals with lymphocytic infiltrates. This was seen in all three patients (H & E, original magnification, ×200).
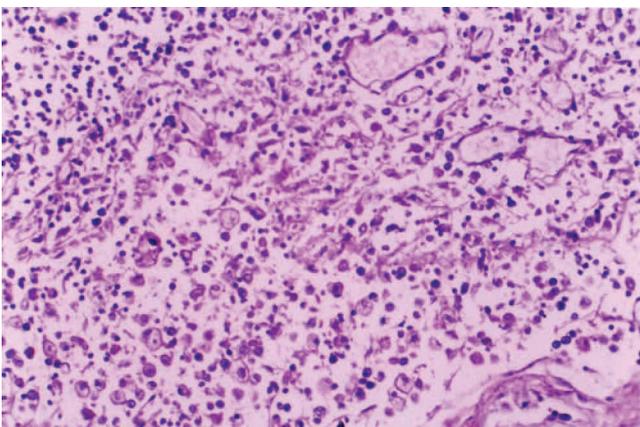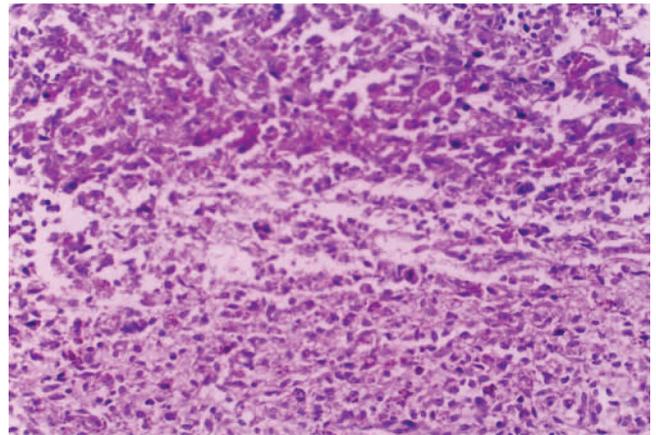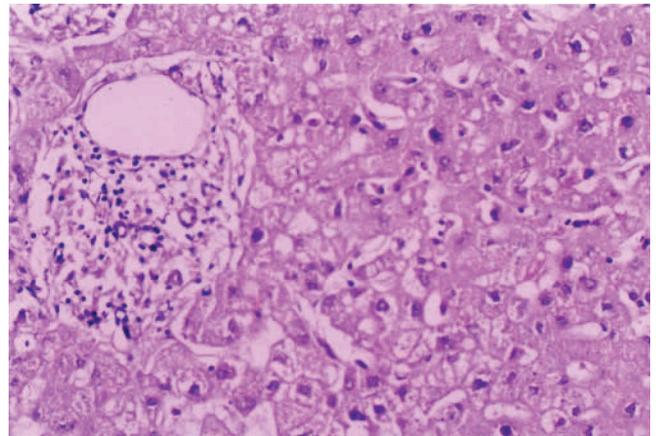

Fig. 7 Lymph node showing loss of structure, expansion of the lymphatic sinuses and blood vessels, loss of cortical lymphocytes and germinal centres (Patient 3). There is macrophage proliferation in the subcapsular sinuses, with lipid vacuoles in the cytoplasm (H & E, original magnification, ×200).
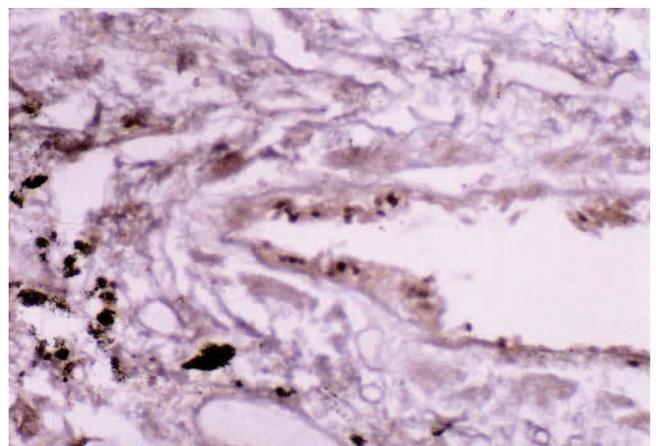

Fig. 10 The positive *in situ* RT–PCR signal for SARS–CoV located in the interstitial cells (×200).

inflammation. Capillary permeability increased markedly as part of the SARS–CoV infection (possibly exacerbated by toxins or coinfection with other pathogens), leading to a leakage of proteins and RBC into the alveolar walls and spaces. There was diffuse alveolar damage, with accumulation of exudate and oedema in alveolar spaces and evidence of hyaline-membrane formation in some alveolar spaces.[2,7–9] These features were present in all three patients, whose length of disease ranged from nine to 15 days, a period of time shorter than in most SARS cases where lung pathology has been reported.[2,5,8,9] Other patients who had lung tissue examined early after disease onset showed similar findings.[9] Giant multinucleated syncytial cells were not seen in this study. These cells were evident in less than half of the patients where lung tissue was collected in the first two weeks of disease.[4,7,9] Cynomologus macaques experimentally infected with SARS–CoV and sacrificed six days post inoculation showed a similar interstitial pneumonia of differing severity.[10] Haemophagocytosis has been reported only occasionally.[9]

A three-stage process has been described with acute respiratory lung disease, including an inflammatory or exudative phase, a proliferative phase, and a final fibrotic phase when the illness is of longer duration.[9,11] The variable degree of exudative inflammation present in different lobes or parts of lobes of the lungs probably represents evolution in the progression of SARS. Other abnormal changes were noted, including hydropic degeneration, fatty degeneration and interstitial cell proliferation that might be caused by the pathogen, or pathogen-induced damage such as hyperpyrexia or hypoxia. The thickened capillary basement membranes, alveolar wall oedema, interstitial cell proliferation, apoptosis and loss of alveolar epithelial cells, exudation, accumulation of proteins and RBC would result in reduced air exchange and oxygenation. Impaired ventilation would result from the bronchiolar hyperaemia and oedema, and the lymphocyte and monocyte infiltration, leading to anoxia, dyspnoea and eventual respiratory failure.

This report confirms that the lung is the main target of the SARS–CoV. In the lung of Patients 1 and 2, virus-like inclusion bodies were observed in pulmonary epithelial cells. These are likely to represent SARS–CoV located in type I and II pulmonary epithelial cells, a feature noted by others.[9] We detected *SARS–CoV* RNA using *in situ* RT–PCR, with positive cells distributed in alveolar epithelial cells, pulmonary interstitial cells and bronchiolar epithelial cells. These are consistent with electron microscopy findings of virus-like particles in lung tissue from patients with SARS.[4,9,12] Others have noted that detection of viral particles is not a constant feature, although this probably reflects the timing of lung tissue sampling.[2,5,7–9]

A novel observation was the damage to pulmonary hilar lymph nodes including loss of lymphocytes in the cortical regions, loss of the germinal centre, and macrophage proliferation in subcapsular sinuses. Splenic changes were similar to the one other report of splenic histopathology,[9] although others have reported only lung involvement.[8]

The SARS–CoV is readily detected by RT–PCR, often for some weeks, in faeces from patients with SARS, although we did not find obvious pathological changes in the gastrointestinal tract. It is possible that different modes of transmission (respiratory, fomites or faecal-oral) may influence the pathological findings in different tissues.

Interpreting the histopathological features of acute SARS is somewhat confounded by the fact that published reports often include only limited autopsies, many patients had been given high-dose corticosteroids, and underlying comorbidities (and pathogens) may have been present.[2,5,7–9] Two of the patients in this study had other medical problems, such as diabetes, hypertension and lung cancer, and one had been given corticosteroid therapy. A number of the pathological features noted here, including renal glomerular hyalinisation and amyloid degeneration of pancreas, were likely to be secondary to diabetes or hypertension. Occasional carcinoma cells were observed in the pulmonary cavity of Patient 1.

Hyponatremia (seen in all three patients) occurs in at least 20% of patients with SARS, and is associated with a poorer outcome.[8,13] The lymphopenia (including CD4+ and CD8+ T-lymphocytes), thrombocytopenia and abnormal liver function tests observed in our three patients are frequent findings in severe SARS.[7,8,13]

The pathological mechanisms of tissue damage and pathogenesis of SARS are being actively pursued. Our data showed that the patients who died relatively early in the illness have acute pulmonary damage, associated with peripheral neutropenia and lymphopenia, and it is likely that these effects are involved in the pathogenesis of SARS–CoV infection. Immunological injury is likely to be of pathologic importance in this disease, as it is in animal coronavirus infections such as feline infectious peritonitis.[14]

Address for correspondence: Professor Lang Zhen-wei, Department of Pathology, Beijing Youan Hospital, Capital University of Medical Sciences, Beijing 100054, China. E-mail: langzw@21cn.com

References

1. Summary table of SARS cases by country (1 Nov 2002 – 7 Aug 2003), Severe Acute Respiratory Syndrome (SARS), World Health Organization Communicable Disease Surveillance & Response (CSR), World Health Organization Website, www.who.int/csr/sars (Date last accessed: 1 September, 2003).
2. Ksiazek TG, Erdman D, Goldsmith C, *et al*. A novel coronavirus associated with severe acute respiratory syndrome. *N Engl J Med* 2003; 348: 1953–66.
3. Drosten C, Gunther S, Preiser W, *et al*. Identification of a novel coronavirus in patients with severe acute respiratory syndrome. *N Engl J Med* 2003; 348: 1967–76.
4. Peiris JSM, Lai ST, Poon LLM, *et al*. Coronavirus as a possible cause of severe acute respiratory syndrome. *Lancet* 2003; 361: 1319–25.
5. Poutanen SM, Low DE, Henry B, *et al*. Identification of severe acute respiratory syndrome in Canada. *N Engl J Med* 2003; 348: 1985–2005.
6. Ruan Y, Wei CL, Ee LA, *et al*. Comparative full-length genome sequence analysis of 14 SARS coronavirus isolates and common mutations associated with putative origins of infection. *Lancet* 2003; 361: 1779–85.
7. Tsang KW, Ho PK, Ooi GC, *et al*. A cluster of cases of severe acute respiratory syndrome in Hong Kong. *N Engl J Med* 2003; 348: 1977–85.
8. Lee N, Hui D, Wu A, *et al*. A major outbreak of severe acute respiratory syndrome in Hong Kong. *N Engl J Med* 2003; 348: 1986–94.
9. Nicholls JM, Poon LLM, Lee KC, *et al*. Lung pathology of fatal severe acute respiratory syndrome. *Lancet* 2003; 361: 1773–8.
10. Fouchier RAM, Kuiken T, Schutten M, *et al*. Koch's postulates fulfilled for SARS virus. *Nature* 2003; 423: 240.

11. Bellingan GJ. The pulmonary physician in critical care: 6. The pathogenesis of ALI/ARDS. *Thorax* 2002; 57: 540–6.

12. Zhao JM, Zhou GD, Sun YL, *et al.* Pathological and etiological findings in a dead case of severe acute respiratory syndrome in China. *Med J Chin PLA* 2003; 28:5 379–82.

13. Booth CM, Matukas LM, Tomlinson GA, *et al.* Clinical features and short-term outcomes of 144 patients with SARS in the Greater Toronto Area. *JAMA* 2003; 289: 1–9.

14. Jacobse-Geels H, Daha MR, Horzinek M. Isolation and characterization of feline C3 and evidence for the immune complex pathogenesis of feline infectious peritonitis. *J Immunol* 1980; 125: 1606–10.